

Automated Optimization Techniques for Phase Change Piezoelectric Ink Jet Performance Enhancement

Paul A. Gilmore
National Science Foundation Industrial Research Associate
Sharon S. Berger and Ronald F. Burr
Color Printing and Imaging Division, Tektronix, Inc., Wilsonville, Oregon
John A. Burns
Director Airforce Center for Optimal Design and Control, Virginia Polytechnical Institute and State University

Abstract

Ink jet printer performance is dependent upon the voltage waveforms driving the jets. As the expected level of printer performance rises, the task of finding suitable waveforms becomes more difficult and time consuming. To allay this problem wa are developing an automated procedure for waveform optimization.

This paper presents several issues relating to this optimization procedure:

- ink jet operation
- drop velocity optimization
- experimental apperatus
- optimization algorithm
- design and results of a reliability and repeatability test
- conclusions and suggestions for further work.

Ink Jet Operation

Figure 1 shows a simplified schematic of an ink jet. A series of voltage pulse waveforms are sent to the Piezo Electric Transducer (PZT). The PZT expands or contracts radially, depending on the sign of the voltage. Expansions of the PZT cause a thin metal sheet (the diaphragm) between the PZT and the pressure chamber to flex outward, thus increasing the size of the pressure chamber. Similarly, contractions of the PZT cause the metal to flex inward, decreasing the size of the pressure chamber. The fluctuations in pressure caused by the expansions and contractions of the metal plate force ink through the outlet and out of the aperture in the form of a drop. Similarly, ink is drawn from the reservoir through the inlet to refill the pressure chamber for the next drop of ink. The drop mass and velocity depend on the metal deflection and hence are functions of the voltage waveform. Thus, by changing the waveform, one can improve (or degrade) print quality.

A typical waveform is indicated in Figure 2. The first (positive) pulse of the waveform expands the PZT, drawing ink into the pressure chamber. The second (negative) pulse contracts the PZT and drives ink through the outlet and out the aperture.

Drop Velocity Optimization

One of the main parameters of ink jet performance is drop velocity. This is true for several reasons:

- Drops with either too high or too low a velocity tend to be unstable.
- When printing an image, jets fire at different frequencies. Typically, drop velocity is dependent on firing frequency. If the difference between drop velocities for different frequencies is too great, image quality is degraded. Hence, it is necessary to find a waveform that minimizes the difference between drop velocities for different firing frequencies.

For these reasons, a major technique for waveform performance evaluation is the frequency sweep. A frequency sweep consists of running a jet over the full range of firing frequencies, from 1(kHz) to the maximum frequency, and recording the distance (d_f) traveled at the nominal flight time for each frequency (f). The maximum frequency varies by printer and print mode. The maximum frequency we use in the single jet is 11(kHz). Typical values for the nominal flight time are 150(μs) to 175(μs).

The parameters currently used to optimize the waveform are shown in Figure 3. They consist of the lengths of the seven time segments $t_0,\ldots,t_6$, and vr, the ratio between the maximum voltages of the first and second pulse. The actual voltage used is determined so that the drop has traveled 25(mils) at the nominal flight time when being fired at 1(kHz). Hence, the voltage is a parameter determined by the waveform variables and is not used as a variable itself.

The merit function used for optimization is

$$L(w) = Max_{f_1,\ldots f_{\max}} \left| \Delta d_{f_i} \right| . \quad (1)$$

In equation (1), w is the vector of waveform variables, $w_0=t_0,\ldots,w_7=vr$, f_i is the ith frequency in the sweep, and

$$\Delta d_{f_i} = \left| d_{f_i} - 25 \right| . \quad (2)$$

Because of both physical limitations (such as the length of time segments must be nonnegative) and a priori knowledge about the effect of waveforms on ink jet performance, each of the variables satisfies $l_i \le w_i \le u_i$. We denote the eight-dimensional hyper-box defined by these constraints by W. The optimization problem we need to solve can now be stated:

$$\underset{w \in W}{\text{Minimize}}\, L(w). \quad (3)$$

Experimental Apparatus and Drop Location

The operation of the system is controlled via a PC through software capable of communicating with both a GPIB (General Purpose Interface Bus) card and a frame grabber card and their associated software. The GPIB card allows the strobe stand software to communicate with the waveform and pulse generators. Through the software, the user can specify the waveform and repetition rate sent to the jet. Each time the waveform generator sends a waveform to the jet, it sends a trigger to the pulse generator, which sends a pulse to an LED. The operator can vary the pulse width and delay of the pulse from the software interface. With each flash of the strobe, a high resolution camera captures the image of a drop. When these images are displayed on a TV monitor it appears as the image of a single drop hanging suspended in the air. The displacement of the drop from the aperture for a specified length of time after firing can be visualized by setting the delay on the strobe to the specified time.

The image from the camera is passed to a Boeckeler video measurement system. This system allows the user to make both horizontal and vertical measurements of objects in the camera's field of view.

Figure 4 shows the image of a drop displayed on the TV monitor, after being passed through the Boeckeler and frame grabber; in this instance, the frame grabber has not altered the image. The number 34.69 is the distance between the vertical Boeckeler lines, measured in (mils). The number 12.9 is the distance between the horizontal lines. The drop is moving from right to left. The center of the drop can be clearly seen left of center, within the Boeckeler lines; also clearly visible is the drop tail. The jet aperture is directly to the right of the drop tail and just to the left of the rightmost vertical Boeckeler line. Above the aperture are several blobs of ink that were splattered out earlier.

After the image is passed through the Boeckeler, it is passed to the frame grabber card. Sending commands to the frame grabber through the software, the user can have the frame grabber capture an image. Regions of the captured image can then be retrieved and manipulated for calculations.

The location of the drop center is calculated as follows:

1 A region containing (hopefully) the image of the drop center is calculated. Except for when the driving waveform causes the jet to be unstable or for high firing frequencies, this region is easy to calculate. For instance, during a frequency sweep, the region used for locating the drop center at a given frequency is an elongated rectangle centered around the drop from the previous frequency.
2 The jet is turned off but the strobe is left firing and an image is captured and stored in the frame grabber. The desired region is brought into the drop location software of the strobe stand and stored as a floating-point array (the jet-off array).
3 The jet is turned on and the process described in step 2 is repeated, creating the jet-on array.
4 The jet-off array is subtracted from the jet-on array. This clears out background problems such as the ink splattered on the front of the jet stack shown in Figure 4.
5 The columns of the resulting array are summed.
6 The column with the largest sum is selected as the drop center.

This method has proven to be very successful in locating the drop center for low to moderate frequencies (less than 12(kHz)). However, at higher frequencies or for unstable waveforms, this method can capture the center of the wrong drop or miss a drop entirely.

Finally after the image is passed through the frame grabber it is displayed on the video monitor for visualization by the user.

Optimization Algorithm

The optimization algorithm is a stochastic variant of the Hooke and Jeeves global optimization algorithm. In the

following discussion, we will assume that W is the unit cube. This causes no loss of generality because the variables can be mapped to the unit cube during use by the optimization algorithm and remapped to their natural values for use by the strobe stand software and hardware. Before we describe the optimization, we define $B(x,s)$ to be the eight-dimensional cube with sides of length s centered at $\boldsymbol{x}$. The optimization has two parts: the box search and the direction search.

The box search goes as follows: given an initial waveform described by the vector w_0, $s \in (0,1]$, and an integer $n > 0$:

1 Randomly generate n points $w_1,...,w_n$ within $B(w_0,s)$, such that $\|w_i - w_j\| \geq 0.2\,s$.

2 Evaluate $L(w_i)$, $i=0,...,n$.

3 Choose $w_{bob} = \underset{i=0,...,n}{Min}\, L(w_i)$ and $w_{wow} = \underset{i=0,...,n}{Max}\, L(w_i)$.

4 Set $w_0=w_{bob}$.

The second part of the optimization, the direction search, depends on data from the box search. The direction search goes as follows:

Given w_{bob}, w_{wow}, $L(w_{bob})$, $L(w_{wow})$, and s:

1 Calculate the approximate directional derivative:

$$Dw = \frac{L(w_{bob}) - L(w_{wow})}{\|w_{bob} - w_{wow}\|}(w_{bob} - w_{wow})$$

2 While $Dw > 0.25\,s$ do the following:

2.1 Calculate $w_t = p(w_{bob} - Dw)$, where

$$p(x) = \begin{cases} 0 \text{ if } x < 0 \\ 1 \text{ if } x > 1 \\ x \text{ otherwise} \end{cases}.$$

2.2 Calculate $L(w_t)$.

2.3 If $L(w_t) < L(w_{bob})$:

2.3.1 Set $w_0=w_t$.

2.3.2 Return.

2.4 Set $Dw=0.5Dw$

In the above description BOB stands for best of the best and WOW stands for worst of the worst. Figure 5 shows a pictorial representation of the combined algorithm.

Global optimization algorithms are designed for finding the global minima (or a close approximation) of a function with multiple minima. Figure 6 indicates that problem (3) is a global optimization problem. The horizontal axes are t_1 and t_5. The vertical axis is the loss function. As can be seen, the surface is rough and contains a number of local minima. The basin of attraction is located in the near right hand corner. The two "spikes" as well as the "ridge" behind them were caused by instability (possibly due to a particle in the aperture) in the jet. Note that the surface falls off after these points for larger values of t_1. Jet instability is just one of the problems that an automated optimization routine must overcome.

Reliability and Repeatability Study

In order to ascertain the performance of the optimization algorithm, a repeatability and reliability (R and R) study was performed. The experiment is outlined below:

- Five waveforms were randomly generated within the constraint hyper-box.
- Starting from these points, the optimization tools were run until the loss function was reduced below 1.7(mils). Then the loss function for the corresponding point was calculated 20 times. If the average was below 1.7, the optimization was terminated; otherwise the optimization was continued.
- Three of the starting points were repeated.
- No fixed method of using the tools was used. The number of points used during the random search, the initial size of the search box, the schedule with which it was contracted or expanded, and the decision whether to do a line search after a random search were all varied throughout the experiment.

The upper and lower bounds for the optimization are shown for each of the waveform parameters in the first two rows of Table 1. The constraints for the box in which the five starting points were randomly generated are contained in the next two rows. The five randomly generated optimization starting points along with their loss function values are shown in the last five rows. The values of the loss function shown for the starting waveforms are the average of 20 evaluations.

The results of the experiment are listed in Table 2. The first eight columns list the optimization variables. The final column contains the average loss function for the final optimized waveform. The first eight rows contain the optimized waveforms. The ninth row contains the average of the optimized waveforms, the tenth row the variance for each variable, the eleventh row contains the standard deviation, and the twelfth row contains the normalized standard deviation for each variable.

The normalized standard deviation is the parameter we use to list the importance of the variables and pulse widths and ratios. The relative importance of each variable is listed in the thirteenth row. As can be seen, the most important variables are t_1 and t_5. This conclusion was supported by a second sensitivity analysis using a larger spread of waveforms.

The effect of the optimization process on t_1 and t_5 is illustrated in Figure 7. As can be seen, the optimization moved t_1 and t_5 into a small region of the hyper-box. The effect of the waveform optimization on drop distance is shown in Figure 8, the drop distance Vs frequency profile for the optimized waveform is much closer to the 25(mils) line than that for the initial waveform. The initial

waveform is the waveform shown in the row labeled "Random Start 2" of Table 1. The final waveform is the waveform shown in the row labeled "Opt wf 7" in Table 2.

As can be seen from Figure 7, the variables t_1 and t_5 were driven into one corner of the hyper-box. To see if the these variables could be pushed further, the bounds on the optimization were changed to $8.0 \le t_1 \le 15.0$, and $18.0 \le t_5 \le 25.0$; the other variables were fixed at the average values given in Table 2. A two-dimensional optimization was run. This optimization is illustrated in Figure 9. The basin of attraction is in the upper-right corner. The initial point was (9.0,19.0). The points generated in the first iterate are shown as dark gray disks. The disk with vertical lines represents w_{wow}, the disk with horizontal lines represents w_{bob}, the dotted line shows the search direction, the arrow indicates the direction search step, and the cross-hatched disk represents the point obtained in the line search. The medium gray disks represent the points obtained in the second iterate and the light gray disks the points obtained in the third. Note that the light gray line search disk is well within the region surrounded by the lowest contour. The loss for this point was 1.2(mils). This optimization run indicates the usefulness of this optimization technique.

Conclusions and Next Steps

- The reliability and repeatability study shows that the optimization code in place in the single jet strobe stand software is capable of optimizing waveforms for drop velocity centering.
- Although not discussed above, the current optimization algorithm appears to be slow (in terms of number of function evaluations). This hypothesis needs to be tested with the introduction of other optimization algorithms such as pattern search methods and genetic algorithms.
- As a parallel development in this project, we plan to introduce optimization algorithms into a numerical model of ink jet behavior being developed at Tektronix. The interplay between optimization on the actual ink jets and optimization on the model will help develop better optimization techniques and will advance the accuracy of the model.

Figure 1:
Ink Jet Schematic

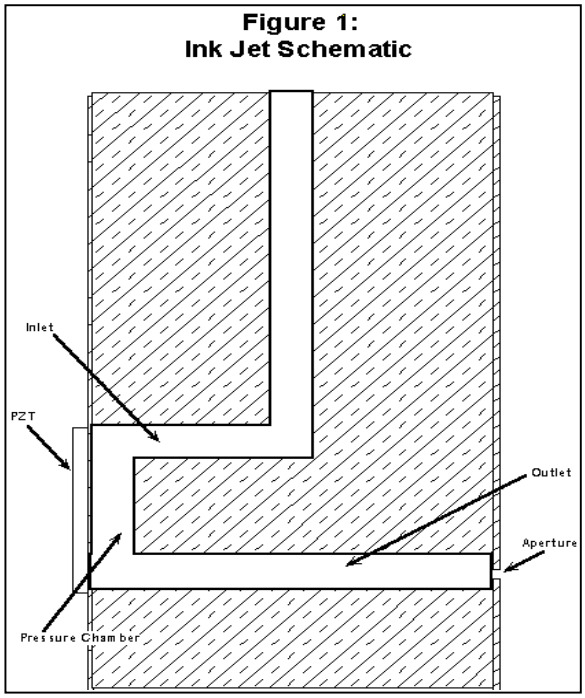

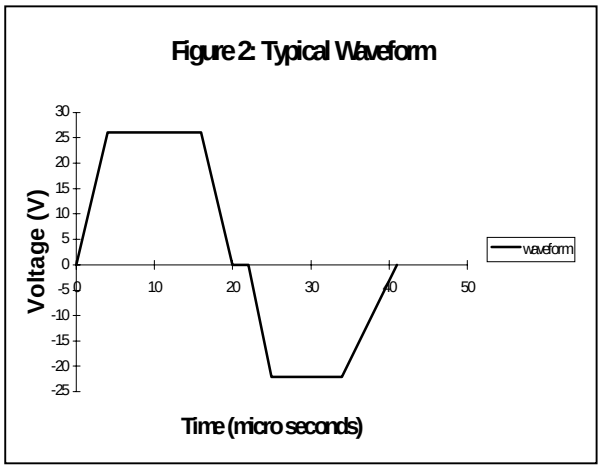

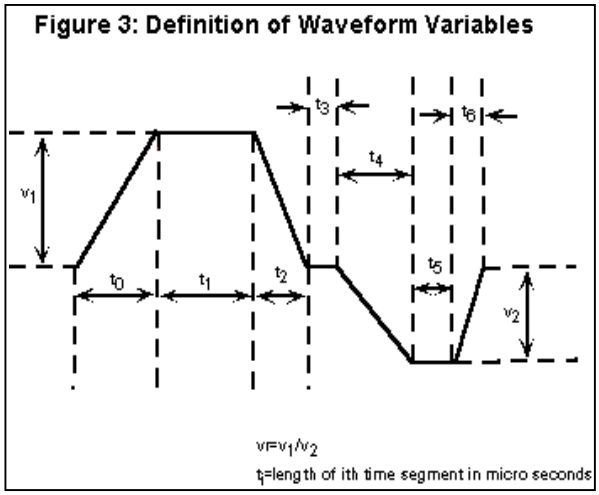

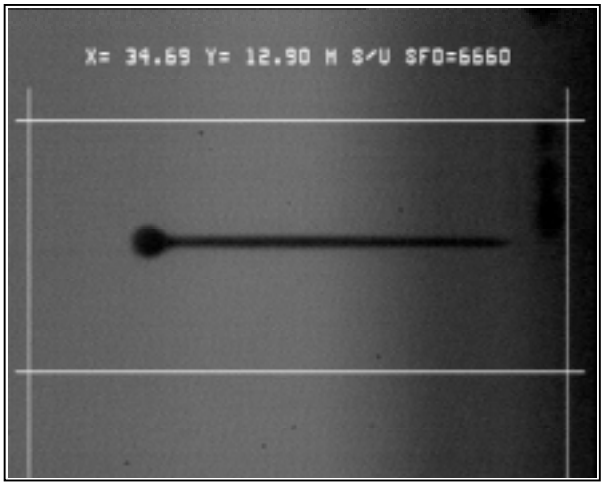

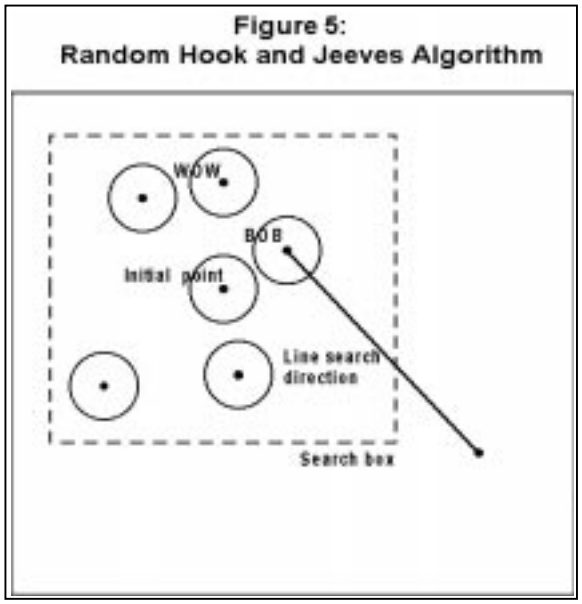

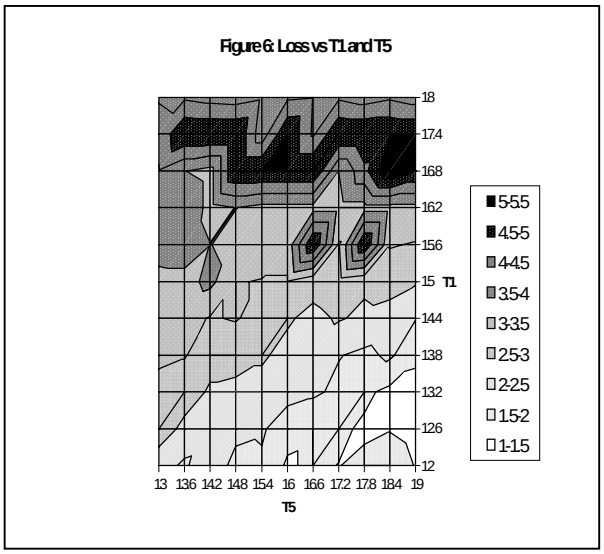

Table 1 Experiment Bounds and Random Starting Points									
	t0	t1	t2	t3	t4	t5	t6	vr	Loss Function
Constraint Lower Bounds	3.0	12.0	3.0	0.5	3.0	12.0	3.0	0.1	NA
Constraint Upper Bounds	9.0	19.0	9.0	3.0	9.0	19.0	9.0	1.0	NA
Generation Box Lower Bounds	4.0	13.0	4.0	1.0	4.0	13.0	4.0	0.3	NA
Generation Box Upper Bounds	8.0	18.0	8.0	2.0	8.0	18.0	8.0	0.6	NA
Random Start 1	6.3	16.2	6.8	1.4	4.3	15.9	6.8	0.4	3.45
Random Start 2	4.9	17.4	6.9	1.5	6.4	16.9	7.6	0.5	3.43
Random Start 3	4.9	16.2	5.7	1.6	4.8	16.4	5.7	0.5	3.73
Random Start 4	4.9	16.0	6.0	1.9	5.9	15.5	4.3	0.4	3.59
Random Start 5	5.5	14.1	7.7	1.5	5.9	13.8	6.1	0.6	3.79

Table 2: Sensitivity Analysis of Optimization Variables

	start point	t0	t1	t2	t3	t4	t5	t6	vr	Loss
Optwf 1	1	7.50	12.00	9.00	2.60	4.50	19.00	8.60	0.39	1.63
Optwf 2	2	3.30	13.30	8.80	1.40	4.90	18.00	9.00	0.27	1.60
Optwf 3	3	3.50	14.20	7.70	2.10	4.80	19.00	9.00	0.31	1.65
Optwf 4	4	9.00	12.00	6.90	0.70	8.90	18.70	9.00	0.42	1.49
Optwf 5	5	8.90	12.00	6.40	2.10	7.30	19.00	5.70	0.49	1.53
Optwf 6	1	8.10	12.00	6.80	0.50	8.90	19.00	8.80	0.31	1.67
Optwf 7	2	4.00	12.60	8.80	0.50	7.20	18.70	8.60	0.31	1.46
Optwf 8	3	3.10	14.00	8.90	2.60	3.80	18.50	9.00	0.30	1.63
average		5.93	12.76	7.91	1.56	6.29	18.74	8.46	0.35	1.58
var		7.14	0.89	1.19	0.82	4.15	0.13	1.28	0.01	0.01
sig		2.67	0.94	1.09	0.91	2.04	0.35	1.13	0.08	0.08
nor sig		0.45	0.07	0.14	0.58	0.32	0.02	0.13	0.22	0.05
importance		7	2	4	8	6	1	3	5